Data-Driven Adaptive Damping Controller for Wind Power Plants with Doubly-Fed Induction Generators

Preprint

Pranav Sharma,[1] Marcos Netto,[2] Venkat Krishnan,[2]
Venkataramana Ajjarapu,[1] and Umesh Vaidya[3]

1 Iowa State University
2 National Renewable Energy Laboratory
3 Clemson University

Presented at the 2021 IEEE Power and Energy Society General Meeting
July 25–29, 2021

NREL is a national laboratory of the U.S. Department of Energy
Office of Energy Efficiency & Renewable Energy
Operated by the Alliance for Sustainable Energy, LLC

This report is available at no cost from the National Renewable Energy Laboratory (NREL) at www.nrel.gov/publications.

Contract No. DE-AC36-08GO28308

Conference Paper
NREL/CP-5D00-78304
July 2021

Data-Driven Adaptive Damping Controller for Wind Power Plants with Doubly-Fed Induction Generators

Preprint

Pranav Sharma,[1] Marcos Netto,[2] Venkat Krishnan,[2] Venkataramana Ajjarapu,[1] and Umesh Vaidya[3]

1 Iowa State University
2 National Renewable Energy Laboratory
3 Clemson University

Suggested Citation
Sharma, Pranav, Marcos Netto, Venkat Krishnan, Venkataramana Ajjarapu, and Umesh Vaidya. 2021. *Data-Driven Adaptive Damping Controller for Wind Power Plants with Doubly-Fed Induction Generators: Preprint*. Golden, CO: National Renewable Energy Laboratory. NREL/CP-5D00-78304. https://www.nrel.gov/docs/fy21osti/78304.pdf.

NREL is a national laboratory of the U.S. Department of Energy
Office of Energy Efficiency & Renewable Energy
Operated by the Alliance for Sustainable Energy, LLC

This report is available at no cost from the National Renewable Energy Laboratory (NREL) at www.nrel.gov/publications.

Contract No. DE-AC36-08GO28308

Conference Paper
NREL/CP-5D00-78304
July 2021

National Renewable Energy Laboratory
15013 Denver West Parkway
Golden, CO 80401
303-275-3000 • www.nrel.gov

NOTICE

This work was authored in part by the National Renewable Energy Laboratory, operated by Alliance for Sustainable Energy, LLC, for the U.S. Department of Energy (DOE) under Contract No. DE-AC36-08GO28308. Funding provided by U.S. Department of Energy Office of Electricity. The views expressed herein do not necessarily represent the views of the DOE or the U.S. Government.

This report is available at no cost from the National Renewable Energy Laboratory (NREL) at www.nrel.gov/publications.

U.S. Department of Energy (DOE) reports produced after 1991 and a growing number of pre-1991 documents are available free via www.OSTI.gov.

Cover Photos by Dennis Schroeder: (clockwise, left to right) NREL 51934, NREL 45897, NREL 42160, NREL 45891, NREL 48097, NREL 46526.

NREL prints on paper that contains recycled content.

Data-Driven Adaptive Damping Controller for Wind Power Plants with Doubly-Fed Induction Generators

Pranav Sharma, *Student Member, IEEE,* Marcos Netto, *Member, IEEE,* Venkat Krishnan, *Senior Member, IEEE,* Venkataramana Ajjarapu, *Fellow, IEEE,* and Umesh Vaidya, *Senior Member, IEEE*

***Abstract*—This paper presents an adaptive damping controller for wind power plants in which the turbines are equipped with doubly-fed induction generators. The controller is designed to respond to an input control signal that is triggered according to the system operating conditions. A processing unit continuously estimates the electromechanical modes of oscillation based on real-time streaming data acquired from a phasor measurement unit that is strategically positioned on the grid. The decision to trigger (or not trigger) the control signal is automatic, based on the relative damping of the dominant mode. The modes are estimated using the dynamic mode decomposition algorithm with time-delay embedding. Numerical simulations performed on the two-area system demonstrate that the proposed controller enhances the rotor angle stability for both small-signal and large disturbances, and is adaptive to changing grid conditions.**

***Index Terms*—Damping controller, doubly-fed induction generator (DFIG), dynamic mode decomposition, Koopman operator, oscillations, real-time control.**

I. Introduction

Electric power grids are transitioning to a future with higher shares of variable renewable generation [1]. One area of concern during this transition relates to the power system's ability to withstand sudden disturbances, including short-circuits and loss of system components. This ability is referred to as the power system dynamic security [2]. Future power systems should be able to maintain or surpass the current standards of dynamic security while allowing for higher shares of variable renewable generation to be deployed. Among the various solutions investigated, some include using synchronous condensers, developing advanced controls for energy storage systems [3], [4] and advancing the flexible operations of variable renewable generation, including wind and solar, for essential reliability services [5]. The present work focuses on advanced controls for wind power plants in which the turbines are equipped with doubly-fed induction generators (DFIGs) [6], that has been widely deployed worldwide. In particular, the objective is to develop an effective controller to counter power system oscillations [7]. Power oscillations damping is arguably one of the most critical real-time control problems in current electric grids, and its importance is going to increase with higher shares of variable renewable generation [8].

The effect on power system oscillations caused by the increase in variable renewable generation and commensurate retirement of conventional synchronous generation is well documented; see, e.g., [9] for an early study. In particular, it has been demonstrated that DFIG-based wind power plants can enhance the damping of power system oscillations [10]; to this end, a wind power system stabilizer (WPSS) can be specifically designed. The WPSS proposed in [10] uses the active power in the DFIG stator as a control input. Other input variables—e.g., the rate of change of the DFIG terminal voltage angle (frequency deviation) as provided by the phase-locked loop [11]—have also been exploited. Note that the control input variables used in [10], [11] are local, and the WPPS design follows the principles used for classic power system stabilizers—hence, their effectiveness in damping inter-area oscillations is limited [12]. To address this limitation, [13] designed a damping controller that incorporates a remote signal in the control input, which is the rotor angle difference between the DFIG and a remote synchronous generator. This control strategy is, however, difficult to implement because wind power plants comprise many DFIGs and individual estimates of rotor angles are not readily accessible. Indeed, any remote control signal is received by a wind power plant through the supervisory control [14]. The supervisory control coordinates the wind turbines within the power plant to achieve system-level control objectives, including reduction of output power variations, voltage control, inertial response, frequency control, and oscillation damping control, to name a few.

In this paper, we start by considering the existence of a supervisory control [14]. Further, we assume that regulations are in place to remunerate the wind power plant for providing oscillations damping control as an ancillary service. This is an important assumption because damping control comes at the expense of operating one or more turbines as part-loaded—with respect to currently available wind capacity—and uses the available power reserve to modulate the power output, which results in a consequent loss of revenue. To implement the proposed adaptive wind turbine control, we use remote measurements of active power to detect the presence of inter-area oscillations, and trigger the adaptive damping from DFIG. This is achieved by processing the measured power data in real-time by supervisory control using the dynamic mode decomposition (DMD) algorithm with time-delay embedding [15]. The DMD algorithm is an emerging methodology to forecast the spatiotemporal evolution of nonlinear dynamical systems and is supported by a strong mathematical foundation revolving around the Koopman operator theory [16].

This paper proceeds as follows. Section II details the proposed adaptive damping controller. Section III describes the power system setup and rationale for the implementation. Section IV discusses the numerical results. Section V provides the conclusions and directions for future research.

II. Adaptive Damping Controller Design

In this section, we set the foundation for the proposed adaptive damping controller for DFIG-based wind power plants. The proposed control scheme is shown in Fig. 1 and is an

This work was authored in part by the National Renewable Energy Laboratory (NREL), operated by Alliance for Sustainable Energy, LLC, for the U.S. Department of Energy (DOE) under Contract No. DE-AC36-08GO28308. Funding provided by the U.S. Department of Energy Office of Electricity (DE-OE0000876). The views expressed in the article do not necessarily represent the views of the DOE or the U.S. Government.

P. Sharma and V. Ajjarapu are with the Department of Electrical and Computer Engineering, Iowa State University, Ames, IA 50011, USA. M. Netto and V. Krishnan are with the National Renewable Energy Laboratory, Golden, CO 80401, USA. U. Vaidya is with the Department of Mechanical Engineering, Clemson University, Clemson, SC 29634, USA. Corresponding author: Pranav Sharma (spranav@iastate.edu).

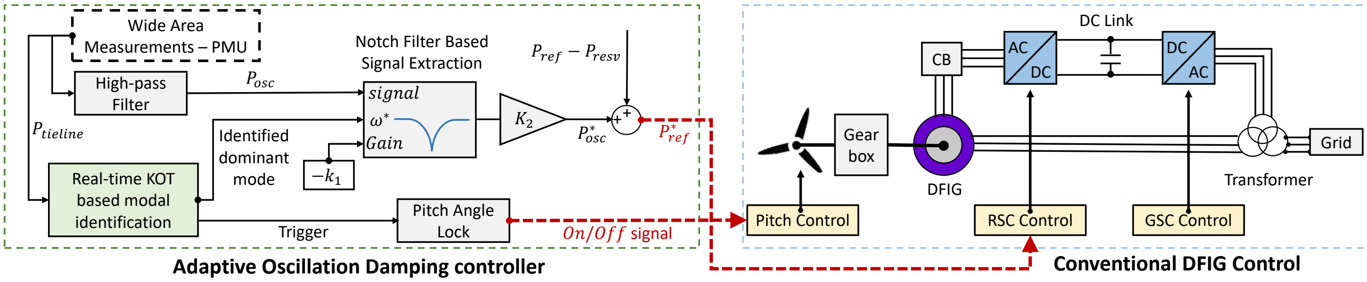

Fig. 1. Proposed adaptive oscillation damping controller implementation

extension of [17]. Remote PMU measurements of the active power flow in a specific tie-line, $P_{tieline}$, are provided as inputs to a high-pass filter and a real-time Koopman operator theory (KOT)-based modal identification algorithm. The former removes the DC component from $P_{tieline}$, while the latter estimates the frequency, ω^*, of the oscillatory inter-area mode. Then, a notch filter extracts the oscillatory component with frequency ω^* from the signal P_{osc} and shifts it by 180 degrees; any other oscillatory component in P_{osc} with a frequency different from ω^* is attenuated. The resulting 180 degrees shifted signal is then superimposed to the initial reference point for the wind turbine and fed into the conventional DFIG control. The KOT-based modal identification block is also used to trigger pitch angle lock based on the damping of the oscillatory mode. Each of these components is discussed in detail in the forthcoming subsections.

A. Conventional DFIG Control

The mechanical torque, T_m, applied by a wind turbine to the DFIG's rotor shaft is given by:

$$T_m = \frac{-P_m}{\omega_r}, \tag{1}$$

$$P_m = \frac{\rho}{2} A_r V_w^3 C_p(\lambda, \beta), \tag{2}$$

where P_m is the mechanical power; ω_r is the rotor speed; ρ is the air density; A_r is the area swept by the rotor blades; V_w is the wind speed; C_p is the power coefficient, which is a function of λ and β; λ is the ratio of the rotor blade tip speed and the wind speed; and β is the blade pitch angle.

The rotor of the DFIG is connected to the grid via power electronics converters—namely, a rotor-side converter (RSC) and a grid-side converter (GSC)—as shown in the right side block in Fig. 1. The GSC controllers regulate the voltage of the DC-link capacitor. The injected current from GSC to the grid, i_g, can be controlled based on the error in the DC-link voltage using a proportional integral (PI) controller. The $d-$axis injected current i_{dg_ref} can be written as:

$$\dot{x}_1 = v_{dc\_nom} - v_{dc}, \tag{3}$$

$$\dot{i}_{dg\_ref} = k_{p1}(v_{dc\_nom} - v_{dc}) + k_{i1} x_1, \tag{4}$$

where x_1 is an internal state for the PI controller, which is a function of error in DC voltage; k_{p1}, k_{i1} are the proportional and integral gain for the controller. v_{dc_nom} and v_{dc} are the nominal and observed DC link voltage respectively. We assign $i_{qg\_ref} = 0$ for zero reactive power injection.

The RSC controllers regulate the active and reactive output power at the rotor terminals. A PI controller is designed to regulate the $q-$axis reference current in the rotor, $i^*_{qr\_ref}$, based on the active power generation error, as follows:

$$\dot{x}_2 = P_{ref} - P_{elec} - P_{loss} \tag{5}$$

$$i^*_{qr\_ref} = k_{p2}(P_{ref} - P_{elec} - P_{loss}) + k_{i2} x_2 \tag{6}$$

where P_{ref} is the reference power and can be obtained as a function of generator rotor speed and input mechanical torque; P_{elec} is the active power in the stator; P_{loss} is the sum of losses caused by mechanical friction, stator heat, rotor heat, and the grid coupling; x_2, k_{p2}, and k_{i2} are, respectively, the internal state, proportional gain, and integral gain of the PI controller. Similarly, a second PI controller regulates the $d-$axis reference current in the rotor based on the reactive power output error. Note that wind power plants are typically designed to operate in maximum active power generation mode.

B. Proposed Control Objective

DFIG-based wind power plants can be designed to provide oscillations damping. To this end, their active power output is modulated such that the active power injected into the grid is in anti-phase—that is, 180 degrees shifted—with existing power system oscillations. Controllers can be specifically designed for damping of local or inter-area oscillations by appropriately choosing the reference point to measure the oscillations. This study focuses on inter-area oscillations, hence, a control block is designed to observe and act on the power oscillations in the tie-lines. The modified reference signal given to the RSC controller is:

$$P^*_{ref} = P_{ref} - P_{resv} + P^*_{osc} \tag{7}$$

where P_{ref} is as previously defined. To provide a buffer for oscillation damping, we reserve headroom P_{resv} from the total capacity of the wind power plant. The buffer requirement can be computed by offline studies of typical oscillation peaks observed in the grid behavior. There is a loss of revenue resulting from the reduction in power generation from wind because typically wind farms are set to generate maximum possible power [14]; however, in the near future, wind power plants will need to participate in ancillary services as well, and market constructs could be in place to monetize such services. For practical implementations, we assume the available buffer value may be communicated by wind power plant owners to independent system operators to participate in the ancillary services market.

C. Real-Time KOT-Based Modal Identification

One key challenge for such a damping controller is to identify the dominant modes present in the system. To this end, we developed a KOT-based modal identification algorithm, which enables us to identify system modes with given measurements. Consider an autonomous dynamical system evolving on a finite, n-dimensional manifold $\mathbb{X}$, as follows:

$$\boldsymbol{x}[k] = \boldsymbol{F}(\boldsymbol{x}[k-1]), \text{ for discrete time } k \in \mathbb{Z}, \tag{8}$$

where $\boldsymbol{x} \in \mathbb{X}$ is the state, and $\boldsymbol{F} : \mathbb{X} \to \mathbb{X}$ is a nonlinear vector-valued map. For such a system, we can define $g(\boldsymbol{x})$ as a scalar-valued function in $\mathbb{X}$, such that $g : \mathbb{X} \to \mathbb{C}$. The function g is referred to as an *observable function*. The space of observable functions is $\mathcal{F} \subseteq C^0$, where C^0 denotes all continuous functions [18]. The Koopman operator, denoted by $\mathcal{K}$ for (8), is a linear, infinite-dimensional operator [19] that acts on g in the following manner:

$$\mathcal{K}g := g \circ \boldsymbol{F}. \tag{9}$$

For the discrete time system (8), the *Koopman eigenvalues*, μ, and Koopman eigenfunctions obey:

$$\mathcal{K}\phi_i = \mu_i \phi_i, \quad i = 1, ..., \infty, \tag{10}$$

where $\mu_i \in \mathbb{C}$, and $\phi_i \in \mathcal{F}$ is nonzero. Now, consider a vector-valued function, $\boldsymbol{g} : \mathbb{X} \to \mathbb{C}^q$. If all elements of $\boldsymbol{g}$ lie within the span of the Koopman eigenfunctions, then for the discrete time system (8):

$$\boldsymbol{g}(\boldsymbol{x}_k) = \sum_{i=1}^{\infty} \phi_i(\boldsymbol{x}_k)\boldsymbol{v}_i = \sum_{i=1}^{\infty} \phi_i(\boldsymbol{x}_0)\boldsymbol{v}_i \mu_i^k, \tag{11}$$

where $\boldsymbol{v}_i \in \mathbb{C}$ are referred to as *Koopman modes* [20].

As shown in the left block of Fig. 1, the proposed KOT-based modal identification block observes the phasor measurement unit (PMU) measurements for power injection at the tie-line buses. This block observes a window of measurements to identify a dominant oscillatory mode of frequency ω^* present in the tie-line and to provide an input to the notch filter. High penetrations of variable renewable generation affect the oscillatory modes of a given power system [9], [21]; hence, a controller with fixed central frequency, ω^*, will not give optimal control for various operating conditions. Therefore, we propose using an adaptive oscillation frequency estimation and notch filter tuning for an adaptive response from the DFIG.

The KOT-based modal identification block also provides an on/off signal to the pitch angle (β) control block. This control design is based on a threshold damping (δ^*) observed for the dominant mode. A change in the power output from the generator leads to a change in the input mechanical torque from the wind turbine. Such oscillations in input torque increase the mechanical wear-and-tear of the wind turbines. Using the pitch angle lock, we fix the input mechanical power to the wind turbine. This acts as a reference power injection for the DFIG and helps avoid introducing any further oscillations of its own while the DFIG tries to modulate its power output to damp out inter-area oscillations.

D. Notch Filter-Based Control Actuation

Notch filters are band-pass filters that are designed to act (amplify or attenuate) on a given central frequency without affecting other frequency components in the signal. For the proposed controller design, we need to extract the components of the dominant oscillatory mode and accordingly provide a damping signal from the wind power plants. For this purpose, a large negative gain ($-k_1$) is used to amplify and invert the signal component corresponding to the central frequency, ω^*. Further, a high-pass filter is also used to provide the signal input to the notch filter. The purpose of this filter is to eliminate the DC component of the tie-line power injection. Finally, a gain is used to normalize the P^*_{osc} signal in per unit of total wind power plant capacity (MW). (*Notch filter parameters: gain*$= -10$*, damping* $= 1$*, wrapping freq* $= 4.189 rad/sec$)

The designed control block is suitable for large power oscillations as well. When the power oscillation peak is greater than the total reserve ($\max |P^*_{osc}| > P_{res}$), then the P^*_{ref} signal will be greater than 1 p.u.; however, the RSC controller has a current saturation block, which will limit the power output to 1 p.u. and clips any oscillatory output beyond its capacity. Therefore, the adaptive damping controller has the capability to damp out large oscillations. A storage interconnected to such wind turbines can further boost such capabilities.

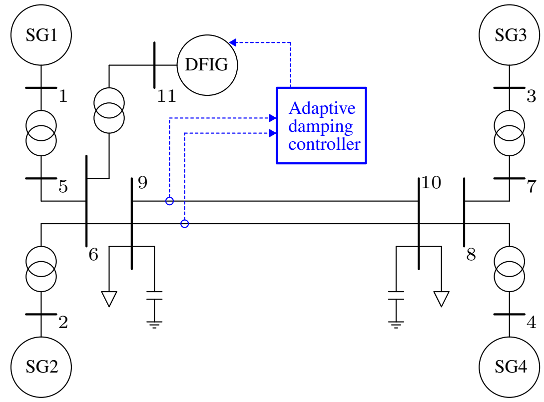

Fig. 2. One-line diagram of the two-area system

To summarize, the proposed adaptive oscillation damping controller will provide two control signals to the conventional DFIG control, as shown in Fig. 1: first, a P^*_{ref} signal to the RSC controller to modulate the power injection from the DFIG; second, a pitch angle lock trigger to the pitch angle (β) controller to fix the mechanical input torque to the wind turbine and avoid oscillations caused by pitch angle controller.

III. Numerical Simulation Studies

A. Case Study: Two-Area System

As shown in Fig. 2, a case study is considered for the two-area system with known cases of inter-area and local modes [22]. The DFIG-based wind power plant is connected in Area 1. A DFIG average model based on GE's 1.5-MW wind turbine [23], [24] developed in MATLAB/Simulink is adopted, as it also provides complete flexibility with control modification. This specific model is suitable for small-signal and transient stability analysis. We consider two wind energy penetration scenarios: 450 MW (approximately 16% of total load) and 1,200 MW (approximately 42% of total load). The adaptive damping controller is designed to mitigate inter-area oscillations in the weakly coupled two-area system and acts on the measurement of $P_{injection}$ at Bus 9. Synthetic PMU measurements with a reporting rate of 100 samples per second are considered for the tie-line flows measuring power injection. A moving window of 100 samples (= 1 s) is fed into the KOT-based modal identification block. Further, to account for the communications and actuation latency, a delay of 0.2 s is considered in control actuation.

The given system has poorly damped inter-area mode; however, with the power system stabilizer (PSS), the system is stable for various operating conditions. In a practical system, synchronous machines equipped with PSS will be present along with the proposed adaptive DFIG controller. For this purpose, we considered a scenario with PSS enabled synchronous generators as the reference case. To evaluate the applicability of the proposed adaptive DFIG control to various events, studies are conducted for: 1) small disturbances, 2) large disturbances including three-phase faults, and 3) scenarios with changing grid conditions.

B. Test 1: Controller Performance for Small Disturbances

The given two-area system has a poorly damped inter-area mode. As shown in Fig. 3, after a small v_{ref} change for one of the synchronous generators at t=30 s, the system undergoes poorly damped oscillations. A suitable PSS can damp out the oscillations within 5 s. The proposed adaptive damping controller further improves the system performance,

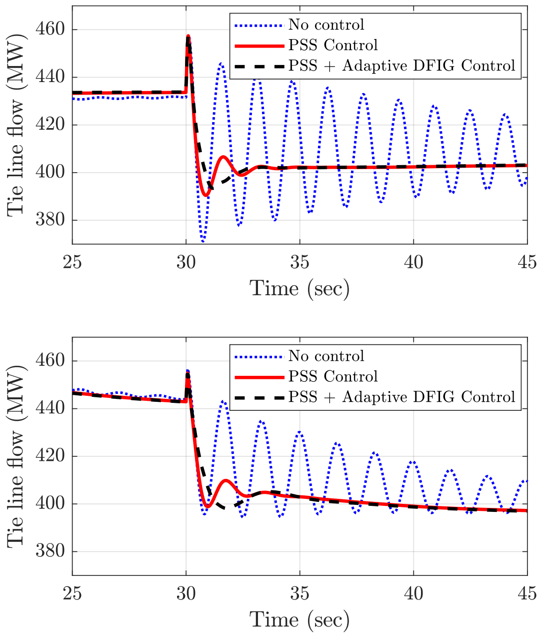

Fig. 3. Tie-line flow from Area 1 to Area 2 after a small disturbance for different control schemes (No control, PSS control, PSS + adaptive DFIG control) (a) for 16% (450 MW) DFIG penetration (b) for 42% (1,200 MW) DFIG penetration

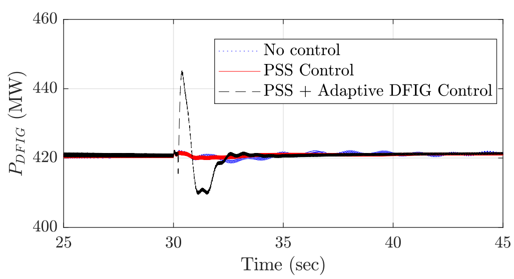

Fig. 4. DFIG response to system oscillations

as reflected by the reduction in the settling time to 3 s. As shown in Fig. 4, the DFIG provides a 180 degree phase-shifted, oscillatory signal to eliminate the oscillations in the tie-line flow. Note that the proposed adaptive damping controller does not violate the performance requirement criteria for the DFIG operations. Here, the instantaneous power output of the DFIG is regulated by changing the P^*_{ref} input to the RSC controller.

To provide a damping control with a 450-MW wind power plant, 6% of the total DFIG capacity is used as reserve. For large wind penetrations (1,200 MW), the fractional share of reserve reduces further to less than 2%. For the small disturbance, the adaptive DFIG controller has similar performance in two different cases of wind penetration. This is because smaller disturbances can still be mitigated with the PSS even with the reduced share of synchronous machines. The impact of high wind penetration is visible for large transient disturbances, as the required control vector is of higher magnitude and the reduction in synchronous generation will hamper the performance of PSS. These observations are discussed in the next subsection.

C. Test 2: Controller Performance for Large Faults

The proposed control is also tested for transient faults in the system. As shown in Fig. 5, for a fault duration of 0.3 s, the PSS alone takes 6.2 s to damp the oscillations. For the same fault, the inclusion of the proposed adaptive DFIG controller reduces the settling time to less than 4 s. The damping controller reduces not only the settling time but also the peak and magnitude of oscillation. The improvement in performance is because of the fast response of power electronic based wind power plants; hence, the designed controller enhances the damping of inter-area oscillations.

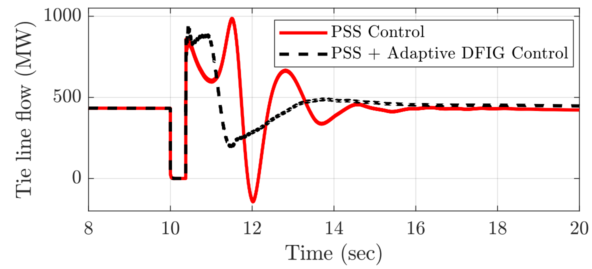

Fig. 5. Tie-line flow for a three-phase fault with and without adaptive DFIG controller for clearing time of 0.3 s

TABLE I
CRITICAL CLEARING TIME FOR A THREE-PHASE SHORT-CIRCUIT AT BUS 9

DFIG penetration (% of net load)	Critical clearing time PSS control only	Critical clearing time PSS + adaptive DFIG control
450 MW (16%)	375 ms	410 ms
1,200 MW (42%)	215 ms	320 ms

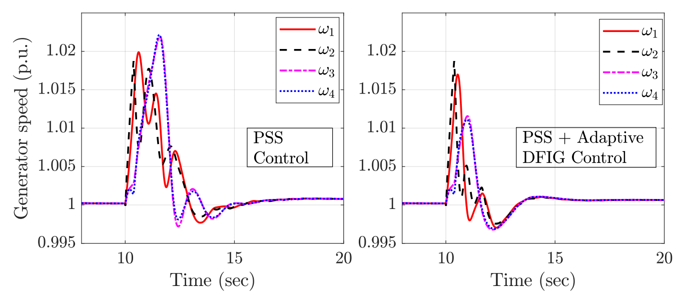

Fig. 6. Synchronous generator rotor speed improvement with adaptive DFIG control for a three-phase fault (a) with PSS control (b) with PSS + adaptive DFIG control

The performance improvement achieved through the adaptive controller increases with increase in share of wind energy in total generation. A detailed study of critical clearing time with different wind penetrations is presented in Table I. For a three-phase line-to-ground fault with 16% DFIG penetration, the critical clearing time improves by 35 ms ($\approx$ 2 cycles). On the other hand, with 42% DFIG penetration, the critical clearing time is improved by 105 ms ($\approx$ 7 cycles). As the share of the synchronous generator decreases, the capability of PSS control to damp the transient oscillations decreases. On the contrary, with a high wind penetration integrated with the proposed adaptive control, the capacity of the wind power plants to damp large oscillations increases.

As such, the oscillation damping controller is designed for oscillations in the tie-line flow; however, the control also reduces the stress on the synchronous machines and the PSS control and improves overall performance. As shown in Fig. 6, rotor speeds for the synchronous generators are synchronized within 4 s with the inclusion of the adaptive DFIG control—as opposed to 8 s with a PSS control alone.

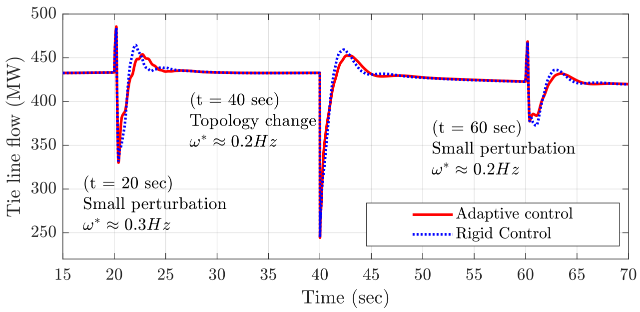

(a)

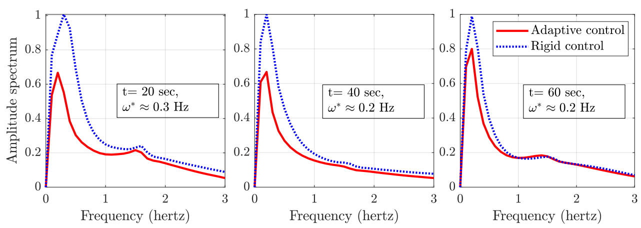

(b)

Fig. 7. Adaptive oscillation damping vs. rigid oscillation damping (a) tie-line flow with three events at t = $\{20, 40, 60\}$ s, and (b) spectrum plot of signal after each disturbance

D. Test 3: Adaptive Real-Time Detection of Multiple Modes and Mitigation

One key feature of the proposed controller is its *adaptive* response to changing grid conditions and oscillatory modes. High penetrations of variable renewable generation induce large variability and uncertainty in system operating points and system modes [9], [21]; hence, it becomes important for the controller to analyze the signal in real time, identify significant modes, and damp them out adaptively.

We compare the proposed adaptive controller with a case where a fixed frequency $\bar{\omega}$ is set for the damping controller. As shown in Fig. 7 (a), the system observes small disturbances at t= s; however there is a topology change at t=40 s. Hence, the dominant inter-area mode (frequency) changes from 0.3 to 0.2 Hz, approximately, and thus the rigid controller based on a fixed frequency input to the notch filter has suboptimal performance. As shown in Fig. 7 (b), the adaptive controller has more effective damping of the system oscillations with variable modes under changing grid conditions.

IV. Conclusion

This paper presents a novel adaptive damping controller for DFIG-based wind power plants. The proposed controller is designed to mitigate oscillatory modes present in the system, similar to the existing PSS-based controls in synchronous machines. The data-driven adaptive controller continuously estimates the electromechanical oscillations present in the system using real-time streaming data acquired from PMUs. Further, an additional pitch angle control is included to mitigate the mechanical wear-and-tear of the wind turbines and avoid local control oscillations while providing an oscillation damping response. The proposed controller improves system performance for small-signal and large disturbances. The results also reflect the effectiveness of the proposed control under high wind penetration scenarios, when synchronous generators with PSS might be retired. In particular, for large disturbances, the improvement in system performance estimated in terms of critical clearing time and oscillation settling time is significant with the proposed adaptive damping controller from the DFIG. The effectiveness of the adaptive nature of the damping controller is demonstrated using a sequence of events, including changing topology and operating conditions, where it proved to be more effective than the traditional deterministic or fixed-frequency control responses. Further research is needed to extend the proposed controller to study the coordination among geographically dispersed wind resources and to understand the control interactions when the wind turbine is used to provide other essential reliability services, such as inertial, frequency, and voltage support.

Acknowledgments

The authors are grateful to Richard Gagnon (Hydro-Québec Research Institute) for his support with the DFIG model.

References

[1] B. Kroposki *et al.*, “Achieving a 100% renewable grid: Operating electric power systems with extremely high levels of variable renewable energy,” *IEEE Power and Energy Magazine*, vol. 15, no. 2, pp. 61–73, 2017.

[2] A. A. Fouad *et al.*, “Dynamic security assessment practices in North America,” *IEEE Trans. Power Syst.*, vol. 3, no. 3, pp. 1310–1321, 1988.

[3] B. P. Roberts and C. Sandberg, “The role of energy storage in development of smart grids,” *Proceedings of the IEEE*, vol. 99, no. 6, pp. 1139–1144, 2011.

[4] A. O. Converse, “Seasonal energy storage in a renewable energy system,” *Proceedings of the IEEE*, vol. 100, no. 2, pp. 401–409, 2012.

[5] V. Yaramasu *et al.*, “High-power wind energy conversion systems: State-of-the-art and emerging technologies,” *Proceedings of the IEEE*, vol. 103, no. 5, pp. 740–788, 2015.

[6] S. Muller, M. Deicke, and R. W. De Doncker, “Doubly fed induction generator systems for wind turbines,” *IEEE Industry Applications Magazine*, vol. 8, no. 3, pp. 26–33, 2002.

[7] G. Rogers, *Power System Oscillations*. Springer, 2000.

[8] T. Sadamoto, A. Chakrabortty, T. Ishizaki, and J. Imura, “Dynamic modeling, stability, and control of power systems with distributed energy resources: Handling faults using two control methods in tandem,” *IEEE Control Systems Magazine*, vol. 39, no. 2, pp. 34–65, 2019.

[9] J. Slootweg and W. Kling, “The impact of large scale wind power generation on power system oscillations,” *Electric Power Systems Research*, vol. 67, no. 1, pp. 9 – 20, 2003.

[10] F. M. Hughes, O. Anaya-Lara, N. Jenkins, and G. Strbac, “A power system stabilizer for DFIG-based wind generation,” *IEEE Trans. Power Syst.*, vol. 21, no. 2, pp. 763–772, 2006.

[11] G. Tsourakis, B. M. Nomikos, and C. D. Vournas, “Contribution of doubly fed wind generators to oscillation damping,” *IEEE Trans. Energy Conversion*, vol. 24, no. 3, pp. 783–791, 2009.

[12] P. Kundur, M. Klein, G. J. Rogers, and M. S. Zywno, “Application of power system stabilizers for enhancement of overall system stability,” *IEEE Trans. Power Syst.*, vol. 4, no. 2, pp. 614–626, 1989.

[13] Z. Miao, L. Fan, D. Osborn, and S. Yuvarajan, “Control of DFIG-based wind generation to improve interarea oscillation damping,” *IEEE Trans. Energy Conversion*, vol. 24, no. 2, pp. 415–422, 2009.

[14] Z. Lubosny and J. W. Bialek, “Supervisory control of a wind farm,” *IEEE Trans. Power Syst.*, vol. 22, no. 3, pp. 985–994, 2007.

[15] M. Kamb, E. Kaiser, S. L. Brunton, and J. N. Kutz, “Time-delay observables for Koopman: Theory and applications,” *SIAM Journal on Applied Dynamical Systems*, vol. 19, no. 2, pp. 886–917, 2020.

[16] Y. Susuki, I. Mezić, F. Raak, and T. Hikihara, “Applied Koopman operator theory for power systems technology,” *Nonlinear Theory and Its Applications, IEICE*, vol. 7, no. 4, pp. 430–459, 2016.

[17] M. Singh *et al.*, “Interarea oscillation damping controls for wind power plants,” *IEEE Trans. Sustain. Energy*, vol. 6, no. 3, pp. 967–975, 2015.

[18] A. Mauroy and I. Mezić, “Global stability analysis using the eigenfunctions of the Koopman operator,” *IEEE Trans. Automatic Control*, vol. 61, no. 11, pp. 3356–3369, 2016.

[19] B. O. Koopman, “Hamiltonian systems and transformation in Hilbert space,” *Proceedings of the National Academy of Sciences*, vol. 17, no. 5, pp. 315–318, 1931.

[20] C. W. Rowley, I. Mezić, S. Bagheri, P. Schlatter, and D. S. Henningson, “Spectral analysis of nonlinear flows,” *Journal of Fluid Mechanics*, vol. 641, p. 115–127, 2009.

[21] R. F. Mochamad, A. Ehsan, and R. Preece, “Probabilistic multi-stability assessment in power systems with uncertain wind generation,” in *2020 International Conference on Probabilistic Methods Applied to Power Systems (PMAPS)*, 2020, pp. 1–6.

[22] P. Kundur, N. J. Balu, and M. G. Lauby, *Power system stability and control*. McGraw-hill New York, 1994, vol. 7.

[23] N. W. Miller, J. J. Sanchez-Gasca, W. W. Price, and R. W. Delmerico, “Dynamic modeling of GE 1.5 and 3.6 MW wind turbine-generators for stability simulations,” in *2003 IEEE Power Engineering Society General Meeting*, vol. 3, 2003, pp. 1977–1983.

[24] R. Gagnon, “Wind farm - DFIG average model,” https://www.mathworks.com/help/physmod/sps/ug/wind-farm-dfig-average-model.html.